




Article

# A Steepest Ascent Analysis Based on an Experimental Approach for the Hardening Process of a Steel Alloy

Paulo Eduardo García-Nava <sup>1</sup>, Gabriel Plascencia-Barrera <sup>2</sup>, Luis Alberto Rodríguez-Picón <sup>1,\*</sup>,  
Roal Torres-Sánchez <sup>2</sup> and Rafael García-Martínez <sup>3</sup>

<sup>1</sup> Department of Industrial Engineering and Manufacturing, Autonomous University of Ciudad Juárez, Ciudad Juárez 32310, Mexico; al206600@alumnos.uacj.mx

<sup>2</sup> Department of Metallurgy and Structural Integrity, Research Center for Advanced Materials, Chihuahua 31136, Mexico; gabriel.plascencia@cimav.edu.mx (G.P.-B.); roal.torres@cimav.edu.mx (R.T.-S.)

<sup>3</sup> Department of Mathematics, University of Sonora, Hermosillo 83000, Mexico; rafael.garciam@hermosillo.tecnm.mx

\* Correspondence: luis.picon@uacj.mx

**Abstract:** A significant number of alloyed metals applied for different purposes are currently available in industry. The hardness of a piece is an important parameter to consider. The tempering process is widely used to change a metal's hardness, which is obtained using a hardness test. Once the response is obtained, a way to evaluate the system is by performing an analysis of variance to verify the significance of terms and obtain a regression equation to improve the response. The aim of this work is to illustrate the implementation of an experimental approach based on the steepest ascent method and stopping rules for optimization purposes by considering the hardening process of the steel alloy 4140. The regression coefficients obtained from an experimental design were used to build the steepest path of improvement. The Myers and Khuri stopping rule and the enhanced parabolic stopping rule were applied to determine the best value while individual experimentation is developed. The obtained results, discussion, and a conclusive analysis are disclosed in this document.



**Citation:** García-Nava, P.E.; Plascencia-Barrera, G.; Rodríguez-Picón, L.A.; Torres-Sánchez, R.; García-Martínez, R. A Steepest Ascent Analysis Based on an Experimental Approach for the Hardening Process of a Steel Alloy. *Mathematics* **2024**, *12*, 3563. <https://doi.org/10.3390/math12223563>

Academic Editors: Carlos Conceicao Antonio and Jüri Majak

Received: 9 September 2024

Revised: 15 October 2024

Accepted: 4 November 2024

Published: 14 November 2024



**Copyright:** © 2024 by the authors. Licensee MDPI, Basel, Switzerland. This article is an open access article distributed under the terms and conditions of the Creative Commons Attribution (CC BY) license (<https://creativecommons.org/licenses/by/4.0/>).

**Keywords:** tempering; steel alloy 4140; hardness test; steepest path; optimization

**MSC:** 62B15; 62K20

## 1. Introduction

Metal alloys are widely studied for a variety of applications due to their different properties. For instance, Zhang et al. [1] explained several recent developments of antibacterial alloys for biomedical materials and the antibacterial mechanisms of alloys for biomedical implants. Additionally, Hoang et al. [2] analyzed the corrosion behavior of alloys in diesel engines due to the biodiesel used. Furthermore, Liu et al. [3] illustrated the characteristics, intrinsic properties, and analytic mechanism of metal-oxide-based nanozymes and their recent applications in biological analysis, relieving inflammation, providing antibacterial therapy, and even improving cancer therapy. Moreover, Fetić [4] studied the effect of the temperature of heat treatment on the microhardness and corrosion behavior of a metallic glass. Similarly, Gloria et al. [5] argued that, recently, a new generation of metals for aeronautics has grown in importance. Additionally, Luo [6] revealed that advanced light metal alloys are widely used in the automotive industry for weight reduction. In addition, Zeng et al. [7] found that magnesium (Mg) alloys have lightweight structural properties and benefits in terms of extrudability, mechanical properties, and microstructural characteristics, resulting in conveniently high performance when applied. It is of great importance to mention that the production process of metal alloys also plays a crucial role in influencing their material properties. For instance, the centrifugal casting process has several effects on the structural stability of metal alloys. He et al. [8] explained that anisotropic behavior was observed in ductile iron pipes due

to the centrifugal casting process, during which the cooling rate is typically faster at the outer surface compared to the inner surface. The authors conducted experiments to investigate the mechanical properties of centrifugal casting ductile iron pipes, emphasizing how sampling orientation, location, preparation, and testing methods affect results. The findings reveal that the mechanical properties of the pipe varied with the wall thickness, being weaker in the internal section and stronger in the middle and external sections. This weaker layer was prone to cracking, which could then propagate outward. They concluded that this inhomogeneity significantly degraded the overall mechanical performance compared to the middle material. Fractographic and metallographic analyses identified casting defects, such as porosity and agglomerated graphite in the internal section, as the main contributors to material inhomogeneity. All in all, the final intention is to reduce costs by expanding the productive life of components. It is crucial to study the most useful metallic alloys, including aluminum, titanium, magnesium, and, of course, steel alloys, that consider recent advancements to effectively reach different objectives.

Particularly, AISI 4140 alloy steel is currently known as one of the most relevant alloys for different specific purposes. Özdemir et al. [9] found that AISI 4140 alloy steel has high abrasion resistance, toughness, torsional strength, and fatigue strength. For example, Gürbüz et al. [10] conducted a study on the effects of different rates and cutting parameters on surface roughness with a significant focus on the machinability criteria and formation of AISI 4140. At the end of the experiments, there was no significant effect on the surface roughness due to these alloy properties. Murwamadala and Rao [11] studied the tribological properties of the AISI 4140 alloy through three tests conducted per sample: rotating, scratch, and reciprocation tests with a lower observed coefficient of friction. Similarly, Borchers et al. [12] compared seven different manufacturing processes (grinding, turning, deep rolling, laser processing, inductive heat treatment, electrical discharge machining, and electrochemical machining) on this alloy inspected by highly specialized examination techniques to evaluate its surface modification (this alloy has a high fatigue strength, toughness, torsional strength, and abrasion resistance).

In addition to these previously mentioned processes, AISI 4140 alloy steel is also widely used for tempering purposes. As is well known, steels are tempered to increase their toughness [13], and they are commonly used in different industrial applications. For instance, Saraç and Altan-Özbek [14] investigated the effects of tempering temperature on the mechanical properties of AISI 4340 and AISI 4140. These steels are normally subjected to hardening processes. Hardness measurements are performed to analyze their mechanical properties and microstructural composition.

There are certain cases where the intention is to look for a maximum or minimum value in the response (hardness) which is obtained by a test measured by the Brinell, Vicker's, or Rockwell scales, determined by the tempering conditions applied. For example, Hu [15] developed a strategy to accurately forecast Vicker's hardness of austenitic steels given certain experimental conditions. This development produced an excellent generalization ability through a validated model to predict the mechanical properties governed by microstructures. Other specialized techniques are currently widely applied to analyze and evaluate response variables such as the hardness of a piece.

Several great tools to evaluate responses are the design of experiments (DOE) and the analysis of variance (ANOVA). This last tool measures the variability of the systems and significance of factors for optimization purposes. For instance, Ali et al. [16] presented the optimization of the key process parameters in electrohydrodynamic atomization through a full factorial DOE for the assessment of various parameters such as voltage, deposition distance, and flow rate. Those results show a significant modification in the morphology of resultant structures with the potential to develop personalized medical devices. Similarly, Smith and Larson [17] described some statistical approaches for the analysis of metal surface in the finishing stage such as full and fractional factorial design of DOE, central composite design, response surface methodology (RSM), and Taguchi methods. Additionally, Moradi et al. [18] optimized a direct laser metal deposition technique in

additive manufacturing using a full factorial design, where the process variables included the laser scanning speed, powder feed rate, and scanning strategies, while the process responses were the geometrical dimensions, standard deviation of microhardness, and the stability of additively manufactured walls. Optimization was achieved and the desired conditions for the additive manufacturing process were applied.

One of the most important stages of a DOE design is the optimization of variables in a process. According to Rao [19], optimization activities focus on obtaining the best possible result under given circumstances to either minimize the effort required or to maximize the desired benefit. The purpose is to find the conditions that give the maximum or minimum value of a function. In the case of metal alloys, such as the steel AISI 4140, optimization activities have been documented with successful results. For instance, Natrayan et al. [20] optimized the tungsten inert gas process parameters using techniques related to DOE. The tensile strength of an AISI 4140 stainless steel welded joint was explored. Different welding process parameters and a regression model were used to establish the correlation between welding input parameters and the penetration of tungsten inert gas welding of AISI 4140 stainless steel plates. The optimal process parameters for tensile strength were successfully reached. Similarly, Özdemir et al. [9] tested AISI 4140 steel specimens using a DOE to find the most effective parameters on its cutting force and surface roughness, with effective results. Moreover, Gürbüz and Emre [21] studied the effects on machinability of AISI 4140 steel by applying different cutting parameters. Furthermore, there was an optimization strategy of cutting conditions through analyses of variance and regression analysis.

The intention of conducting this type of analysis and procedures in several types of industries relies on the importance of finding the maximum possible observed response by using specific statistical methods. In this case, the purpose of this work is to present a study of a hardening process of the steel alloy 4140 for maximization purposes. This alloy is frequently used for many purposes; finding a maximum response in its hardness constitutes a task of high importance when the final product requires such property.

The distribution of this work is divided into seven sections. This first section, the introduction, mentions a brief overview of metal alloys (including the steel alloy 4140) and examples of tempering processes and their analysis through a statistical approach. The second section concerns the steepest ascent or descent methodology (SADM). The third section describes the method, the materials, and the characteristics of the experiment developed. Section 4 shows the results of the analysis. Section 5 presents a brief discussion of the findings. Finally, Section 6 presents a conclusion of the entire document.

## 2. The SADM and Its SRs

SADM is used as the base to reach a response area where an optimization is feasible. According to Myers et al. [22], SADM constitutes an experimental design, model-building procedure, and sequential experimentation scheme in the search for a region of improved response. This is achieved by sequential increments of the factors from one region to another in more than one experiment. Nevertheless, the number of individual experiments applied to make an improvement might be not accurate and the cost of the resources used may be high and not affordable. For this reason, researchers commonly use proper procedures to stop experimentation, with mathematical justification to prevent a waste of experimentation resources. These procedures are known as stopping rules (SRs).

On the one hand, Myers and Khuri [23] first proposed the Myers and Khuri stopping rule (MKSR). This rule assumes that the behavior of the observed response  $y(t)$  is normally distributed such that  $y(t) \sim normal(\eta(t), \sigma^2)$ . It applies a significance test using a confidence interval, the solution for the limits of the interval is given by  $a$  and  $b$ ; then, the next consideration is followed:

Experimentation continues if  $y(n_i) - y(n_i - 1) \geq b$  or  $y(n_i) - y(n_i - 1) < b > a$ .  
Experimentation stops if  $y(n_i) - y(n_i - 1) \leq a < 0$ .

In this case,  $y(n_i)$  is the present value of the response variable at the  $n_i$  step in the SADM improvement path,  $y(n_i - 1)$  is a previous response in the improvement path, and  $a$  is an interval limit for the test of significance. Then, a solution for  $a$  and  $b$  limits is established with  $a = -b = \phi^{-1}(\frac{1}{2\kappa})(\sigma_\epsilon)(\sqrt{2})$ , where  $a$  and  $b$  are the interval limits of the significance test,  $\Phi$  is a cumulative distribution function of the normal,  $\kappa$  is an assumption of the number of individual experiments to run to reach an improvement, and  $\sigma_\epsilon$  is the square root of the adjusted mean square of the ANOVA in the factorial analysis. It is part of the procedure to return to  $t^*$  such that  $Y(t^*) = \max_{l=1, \dots, t} \{Y(l)\}$ .

On the other hand, Miró-Quesada and Del Castillo [24] proposed the enhanced recursive parabolic stopping rule (ERPSR), which poses an improvement of its predecessor recursive parabolic stopping rule (RPSR) [25]. The enhanced rule recursively fits the second-order term to assume a quadratic behavior in the response, but it also fits the first-order terms to make it less sensitive to a quadratic behavior and more robust to a possible linear behavior in the observed response in  $y(t) = \eta(t) + \epsilon_t = \theta_0 + \theta_1 t + \theta_2 t^2 + \epsilon_t$ .

This procedure is summarized in five main steps:

1. The procedure increases its robustness by fitting the response to also assume non-quadratic behavior. It is performed by specifying a maximum number of individual experiments in the recursive least squares algorithm used in this SR. A concept called "window" must be applied to locally fit the parabolic model along the search direction to make it less sensitive to a large amount of scaled deviation from quadratic behavior. The window size ( $N$ ) is determined using an indicator called the signal-to-noise ratio (SNR). This is estimated by the equation  $SNR = \frac{\|b\|}{\sigma_\epsilon}$ , where  $\sigma_\epsilon$  is the standard deviation of the central points of the experiment. The variable  $\|b\|$  is estimated using the next equation, given as  $\|b\| = \|\beta\| = \sqrt{\sum_{i=1}^k b_i^2}$ . Consecutively, it is necessary to identify  $N$  in a table of values given by [24] with the window sizes for all  $t < N - 1$ , so it becomes possible to identify  $N \times 1$ , the vector  $b_N$ , and the scalar  $\sqrt{v_N}$ .
2. An initial guess is proposed about the number of individual experiments believed to be needed to reach the optimum. Additionally, a parameter estimation when  $t = 0$  is computed using  $\theta_0^{(0)} = Y(0)$ ,  $\theta_1^{(0)} = \|b\|$ , and  $\theta_2^{(0)} = -\frac{\theta_1^{(0)}}{2 * t_{prior}}$ . The notation  $Y(0)$  represents the arithmetic mean of the responses obtained by the center points of the experiment. The notation  $\|b\|$  represents the square root of the sum of the squares of the regression coefficients of the linear model of the experiment.
3. The algorithm makes use of the defined matrix a:  $\theta^{(t)} = \begin{bmatrix} \theta_0^{(t)} \\ \theta_1^{(t)} \\ \theta_2^{(t)} \end{bmatrix}$ , matrix b:  $\phi_t = \begin{bmatrix} 1 \\ t \\ t^2 \end{bmatrix}$ , matrix c:  $\frac{d\phi_t}{dt} \equiv d_t = \begin{bmatrix} 0 \\ 1 \\ 2t \end{bmatrix}$ , and matrix d:  $P_0 = \begin{bmatrix} 1 & 0 & 0 \\ 0 & 1 & 0 \\ 0 & 0 & 10 \end{bmatrix}$  for updating parameters  $\theta_0$ ,  $\theta_1$ , and  $\theta_2$ . Matrix  $P_0$  works as the identity matrix; the value of 10 given in the position of its third column and third row makes the procedure more robust against possible discrepancies between  $t_{prior}$  and  $t^*$ , providing "adjustment" capacity to the variable curvature. Then, for the recursive calculation of  $\theta^{(t)}$ , the equation  $\theta^{(t)} = \theta^{(t-1)} + \frac{P_{t-1}\phi_t}{1 + \phi_t' P_{t-1} \phi_t} + * (Y_{(t)} - \phi_t' \theta^{(t-1)})$  is updated and, to update  $P_t$ ,  $P_t = Var(\theta^{(t)}) / \sigma_\epsilon^2 = (I - \frac{P_{t-1}\phi_t}{1 + \phi_t' P_{t-1} \phi_t} \phi_t') P_{t-1}$  is calculated.
4. The decision rule  $d'_t \theta^{(t)} < -1.645 \sigma_\epsilon \sqrt{d'_t P_t d_t}$  is applied for  $t < N - 1$ .
5. When the decision rule is satisfied, the experiment stops, and that response is considered to be the best. If a better response is identified earlier, that value becomes the best new response. It means that we return to  $t^*$  such that  $Y(t^*) = \max_{l=1, \dots, t} \{Y(l)\}$ .

As previously said, the MKSR assumes that the behavior of the observed response  $y(t)$  is normally distributed; this means that it considers that the response will have a linear behavior, while the ERPSR assumes that the response is quadratic, but it fits the first-order

term of its model to make it less sensitive to a quadratic behavior and more robust to a possible linear behavior. This means that it has the capability to assume that the response can have both quadratic and linear behavior. Nevertheless, an innovative way to improve the response of this study case and offer a new perspective on the problem of optimizing steel tempering processes is by adapting the analysis to the response variable of the study case without the need to assume its behavior to be linear or quadratic. This optimization strategy is related to a stopping rule called the adaptive sequential stopping rule (ASSR) [26]. This rule is based on the Wiener process; it considers the drift parameter as a component of adaptability to any behavior that an experimental response may build. Also, the drift is well described as the rate of change or variation between stochastic trajectories. Moreover, if a rate function is capable to characterize the nature of the behavior of the trajectory, it will efficiently determine a maximum desired response in the process. It uses a Bayesian inference modeling scheme to sequentially estimate the parameters involved. Also, it is based on the definition of a confidence interval for a future observation estimation using the same rate function previously mentioned in search of an optimal response. This adaptive stopping rule has ten general steps:

1. Perform an experiment on  $t_j, j = 1, 2, \dots, n$  to obtain the observation  $y(t_j)$ .
2. Obtain  $\Delta y(t_j) = y(t_j) - y(t_{j-1})$  starting from the second individual experiment.
3. Consider a sample size of  $m = 5$  for  $\Delta Y^{(k)}(t_j)$ .
4. Assume that  $\Delta Y^{(k)}(t_j)$  is described by a Wiener process.
5. Incorporate the Hjorth rate and its parameters  $\beta, \delta$ , and  $\theta$  to the Wiener process.
6. Model the experimentation scheme with Bayesian inference using the software OpenBUGS version 3.2.3 rev. 1012 to estimate the parameters  $(\delta, \theta, \beta, \sigma)$  for each  $\Delta Y^{(k)}(t_j)$ .
7. Obtain the parameter set  $(\hat{\delta}^{(k)}, \hat{\theta}^{(k)}, \hat{\beta}^{(k)}, \hat{\sigma}^{(k)})$  for each  $\Delta Y^{(k)}(t_j)$ .
8. Characterize the shape of the trajectory for each set  $\Delta Y^{(k)}(t_j)$  according to  $(\hat{\delta}^{(k)}, \hat{\theta}^{(k)}, \hat{\beta}^{(k)})$ .
9. Calculate the upper limit of a confidence interval to estimate the maximum future increment using  $UL_{(\Delta Y^{(k)}(t_j)|\delta, \theta, \beta, \sigma \sqrt{\Delta t})} = Y_0 + \left( \hat{\delta}^{(k)} + \frac{\hat{\theta}^{(k)}}{(1 + \hat{\beta}^{(k)})} \right) (t_{j+1}) + 1.96 \hat{\sigma}^{(k)} \sqrt{(t_{j+1})}$ .
10. Decide when to continue or when to stop experimenting using the following decision rules:

Experimentation stops if  $Y_0 + \left( \hat{\delta}^{(k)} + \frac{\hat{\theta}^{(k)}}{(1 + \hat{\beta}^{(k)})} \right) (t_{j+1}) + 1.96 \hat{\sigma}^{(k)} \sqrt{(t_{j+1})} \leq 0$  when  $Y_0$  is negative, or  $Y_0 + \left( \hat{\delta}^{(k)} + \frac{\hat{\theta}^{(k)}}{(1 + \hat{\beta}^{(k)})} \right) (t_{j+1}) + 1.96 \hat{\sigma}^{(k)} \sqrt{(t_{j+1})} = Y_0$  when  $Y_0$  is positive.

A detailed description and explanation of the method is presented by García-Nava and Rodríguez-Picon [26].

For this paper, the MKSR is used because of its assumption of linearity in the experimental response, the ERPSR is used because of its assumption of both quadratic and linearity in the experimental response, and, finally, the ASSR is used because of its capability of adaptation to the experimental response. At the end of this analysis, the outcome will determine which SR performs better under the same circumstances.

### 3. Materials and Methods

This document presents a case study related to a steel tempering process. The method used is described in this section. The motivation that a professional may have when developing this kind of analysis comes from the need to optimize resources. This means working in optimal conditions by systematically varying factors to determine the best settings to achieve desired outcomes. In this case, the experiment is carried out to maximize the hardness (response) of the material (steel alloy 4140). Maximizing the hardness of this steel alloy is important, particularly in applications where high strength and wear resistance are critical. Hardness is important because it improves the alloy's resistance to wear and abrasion, the material's lifespan can be extended, it helps in maintaining precise



dimensions and tolerances, and it can contribute to better performance characteristics. This paper first develops a screening experiment using DOE to apply the RSM and build a path of improvement. Finally, the objective is to maximize the response.

The method is shown in Figure 1. Different factors and levels were used in this tempering experiment to build a  $2^k$  factorial design. The mathematical model was fitted to build a path of improvement using SADM and optimize the response (the hardness of the alloy). Finally, the SRs mentioned were applied to determine the moment to stop individual experimentation over the steepest direction.

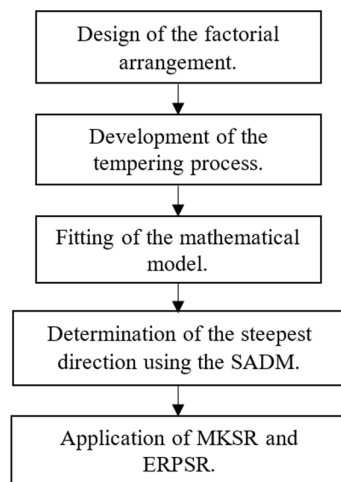


**Figure 1.** Proposed method for the analysis of the case study.

### 3.1. Design of the Factorial Arrangement

The experiment is a full factorial design that includes 2 factors with 2 levels for each factor, so it is explained by a design of  $2^2 = 4$  runs. The design has 2 replicates, 2 blocks, and 2 center points per block. As seen in Table 1, the total of applied runs is 12.

**Table 1.** Full factorial design summary.

Summary of Design			
Factors:	2	Base Design:	2, 4
Runs:	12	Replicates:	2
Blocks:	2	Center pts (total):	4

A common tempering process consists of heating a piece and suddenly cooling it. It allows an increase in the hardness of the metal. The two factors considered for this tempering process were the temperature of the furnace and the exposition time for cooling. The blocks involved are related to two types of cooling environment: oil and water. The level of the temperature ranges from 825 to 880 °C and center points of 852.5 °C. The levels of the exposition time for cooling ranges from 5 to 95 s and center points of 50 s.

### 3.2. Development of the Tempering Process

The pieces were first cleaned and sanded. The device shown in Figure 2 was used to polish pieces. Once pieces were polished, the tempering process could be properly developed.

After this, pieces entered the furnace (Figure 3) according to temperatures from factorial design. Special equipment must be used in the laboratory because the furnace manages excessive temperatures in the process.



Figure 2. Device used to sand pieces.

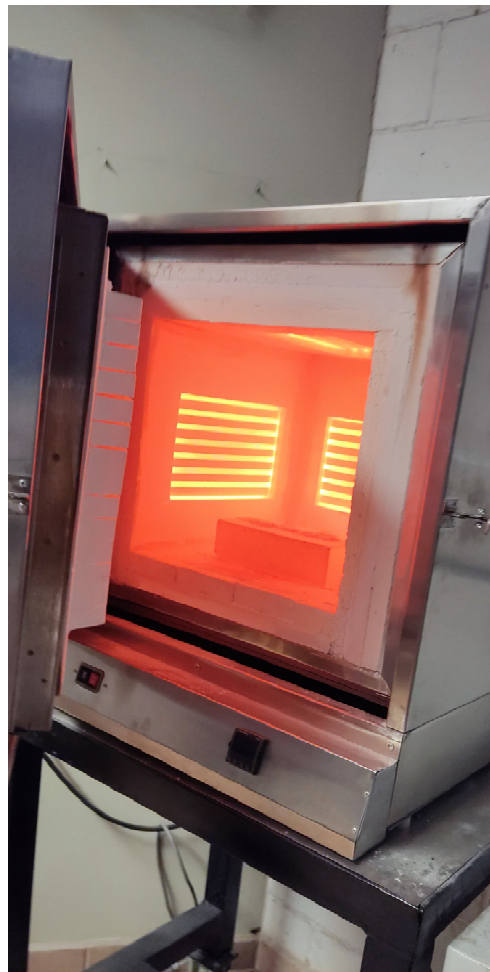


Figure 3. Furnace used in operation.

Then, the pieces were introduced in oil and water, as shown in Figure 4, according to the blocks of the factorial arrangement.



**Figure 4.** Cooling environment used.

After the pieces were cooled under specific cooling conditions, they were subjected to a hardness test. This value is used as the response variable of the factorial design. The device used for this test is the one shown in Figure 5. Rockwell HRB and Rockwell HRC were the scales used for measurements; later, all values were converted into Vickers (HV) to manage only one type of scale, and so that the data could be analyzed.

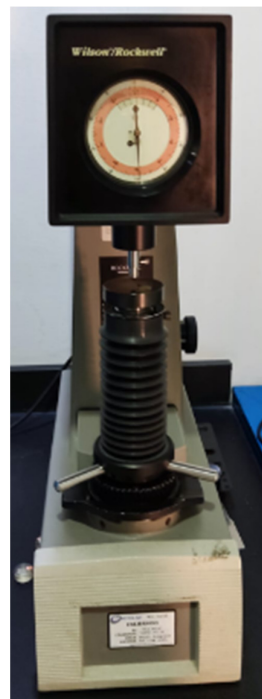


**Figure 5.** Metal alloy 4140 Metrolab hardness tester.

A total of five test points per piece were applied, as shown in Figure 6. The arithmetic mean of the values was used in each piece for the data analysis.





**Figure 6.** Hardness test points applied to the specimen.

The microstructure and hardness of the steel alloy 4140 are significantly influenced by temperature and time. On the one hand, the temperature is crucial: the way the specimen is heated and cooled transforms the microstructure. For example, carbon atoms can dissolve more readily in iron (Fe), leading to a complete changing of structure. Rapid cooling transforms the material into a very hard structure. On the other hand, time is also important: the time the steel is held at high temperature affects the transformation. For instance, if there is insufficient time, not all the microstructure may change, but if there is an excessive time of exposure, it can lead to grain growth, reducing the hardness and strength of the material due to thicker microstructure.

Other parameters are related to the tempering process of the alloy 4140. It contains carbon, chromium, and molybdenum, which increase the ability of transformation of the specimen. Higher content typically results in higher hardness after the tempering process. The parameters considered for this experiment were properly referenced and selected for the scope and intention of this paper.

In order to make the impact of this paper clear for real-world applications, an industry benchmark is presented. According to Khani et al. [27], the material microstructure and mechanical properties of steels have been of interest in metallurgy. It is well known that quenching and tempering are expected to improve both strength and toughness of specimens. Iranian Alloy Steel Co. (Yazd, Iran) developed an AISI 4140 steel by melting steel refined by various methods to reduce the level of impurities such as sulfur and phosphorous. The chemical composition of their AISI 4140 steel is shown in Table 2.

**Table 2.** Chemical composition of AISI 4140 from Iranian Alloy Steel Co.

%C	%Si	%Mn	%P	%S	%Cr	%Mo	%Fe
0.42	0.2	0.79	0.014	0.023	1.07	0.185	Balance

The experiment developed by [27] using steel alloy 4140 represents a benchmark for the experiment presented in this paper in three different ways:

1. Both experiments considered heating temperatures, time in the furnace, cooling rate, and cooling medium. On the one hand, the heating temperatures on both experiments range from 860 to 880 °C and the time in the furnace ranges from 60 to 120 min. On the other hand, the cooling rates are in a range of seconds, and the cooling medium in water and oil causes a thermal shock that benefits the physical change of the piece.
2. Khani et al. [27] mentioned that sudden cooling in the heat treatment process resulted in a significant improvement of properties related to hardness performance. This sup-

ports the cooling time and cooling environment stated in this paper. The alloying elements of the material would not constitute a variable because they are fixed.

3. Optical metallography of the specimen helps us to visualize the grain distribution of the steel alloy 4140. The metallography used in both experiments is similar.

After the development of the tempering process and obtaining the statistical information, we fit the mathematical model.

### 3.3. Fitting of the Mathematical Model

The fitting of the model is explained by the coded coefficient table from the statistical analysis shown in the Results section. Once the equation is built, it is known as regression equation of coded units (RECU). The form of the mathematical model is shown in Equation (1).

$$\hat{y} = b_0 + b_1x_1 + b_2x_2 + b_3x_1x_2. \tag{1}$$

where

- $\hat{y}$  = estimated response;
- $b_0$  = constant or intercept;
- $b_i$  = coefficient of term;
- $x_i$  = variable or term.

The Results section shows the way this equation was obtained from the coded coefficient table and the way it was used for the rest of the improvement procedure.

### 3.4. Determination of the Steepest Direction Using the SADM

The SADM consists of three steps:

1. First, a step size is chosen in one of the process variables to be used as the main  $\Delta x_i$ . Typically, the most known variable is selected, or the variable that has the largest absolute magnitude in its regression coefficient  $|b_i|$  is selected.
2. The step size for the ascent or descent path for the other variable is calculated using Equation (2).

$$\Delta x_j = \frac{b_j}{b_i/\Delta x_i}; \text{ for } j = 1, 2, \dots, k, \text{ and when } i \neq j. \tag{2}$$

where

- $\Delta x_j$  = coded step size for factor  $x_j$ ;
- $\Delta x_i$  = coded step size for factor  $x_i$ ;
- $b_j$  = regression coefficient of the considered factor  $x_j$ ;
- $b_i$  = regression coefficient of the selected factor  $x_i$ .

3. Finally,  $\Delta x_j$  from coded variables is converted into natural units.

It is important to set an appropriate value for  $\Delta x_i$ . Therefore, it will be possible to build a better path of improvement and a proper sequential increment of levels.

### 3.5. Application of MKSR, ERPSR, and ASSR

As previously said, the MKSR applies a significance test using a confidence interval, and the solution for the limits of the interval  $(a, b)$  is given by  $a = -b = \phi^{-1}\left(\frac{1}{2\kappa}\right)\sigma_\epsilon\sqrt{2}$ . This interval constitutes a range of the difference between two individual observations. Correspondingly,  $\phi^{-1}$  is the standard inverse cumulative function of the normal distribution,  $\kappa$  is a guess of the number of individual experimentation runs to arrive to the improvement, and  $\sigma_\epsilon$  is the square root of the adjusted mean square or the experimental error. The significance test (3) is presented as follows:

$$y(n_i) - y(n_{i-1}) \leq a < 0. \tag{3}$$

In this case,  $y(n_i)$  represents the present response value in the path of improvement and  $y(n_{i-1})$  is the previous response value in the steepest direction. If Equation (3) is fulfilled,

experimentation stops and the response  $\hat{y}$  returns to  $t^*$  such that  $y(t^*) = \max_{(l=1, \dots, t)} y(l)$ . Otherwise, experimentation continues if  $y(n_i) - y(n_i - 1) \geq b$  or  $y(n_i) - y(n_i - 1) < b > a$ .

Now, the ERPSR fits the second-order term in  $y(t) = \eta(t) + \varepsilon_t = \theta_0 + \theta_1 t + \theta_2 t^2 + \varepsilon_t$  to assume a quadratic behavior in the response of individual experimentation obtained from the steepest ascent path. It applies a concept known as “window” to only fit a portion of the quadratic model along the steepest search to make it less sensitive to parabolic behavior. Then, it recursively fits the estimation of the different parameters  $\theta_i^{(t)}$  to apply the decision rule (4) for  $t < N - 1$ .

$$d'_t \theta^{(t)} < -1.645 \sigma_\varepsilon \sqrt{d'_t P_t d_t} \tag{4}$$

If Equation (4) is fulfilled, experimentation stops and the response  $\hat{y}$  returns to  $t^*$  such that  $y(t^*) = \max_{(l=1, \dots, t)} y(l)$ .

### 4. Results

The full factorial design illustrates the two blocks applied as the cooling environment of the piece (water and oil), the factor  $x_j$  (the furnace temperature in °C), and the factor  $x_i$  (the exposition time for cooling in seconds). It includes the responses shown in HV hardness units. The validity and reliability of the experiment is explained by the formal  $2^k$  design used that additionally incorporates two replicates, two blocks, and two center points per block. The scope of this experiment is explained in the framework of these 12 runs offered within the levels and factors experimented. Factorial design and hardness values expressed in the HV scale are shown in Table 3 according to the factorial design.

Table 3. Full factorial design with hardness values.

	Blocks	Run	Furnace Temperature (°C)	Cooling Time (s)	Vickers (HV) Hardness
Water	2	1	880	5	402
	2	2	852.5	50	454
	2	3	825	95	479
	2	4	880	95	483
	2	5	852.5	50	454
	2	6	825	5	398
Oil	1	7	852.5	50	452
	1	8	825	95	475
	1	9	880	5	397
	1	10	852.5	50	453
	1	11	880	95	480
	1	12	825	5	395

This experiment not only offers the combination of levels of the factors in each of the two blocks, but it also illustrates the response variable of the experiment (hardness). The factors selected and the ranges of the levels from both factors (furnace temperature and cooling time) constitute the current scope of this experiment.

The contour plot of the experiment is illustrated in Figure 7. The contour lines help to visualize the way the variable changes across a two-dimensional space. Each contour line represents a specific level of response. The spacing between lines indicates the gradient; closely spaced lines suggest steep changes, while widely spaced lines indicate gentle slopes. Specifically, it can be noted that the highest response can be found at the upper right corner, where the highest levels from both factors define this response.

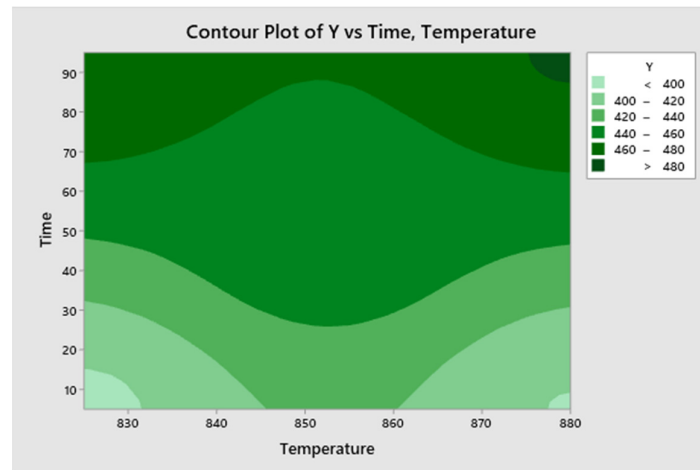


Figure 7. Contour plot of the experiment.

The developed tempering process includes metallography. The illustrations of the pieces that explain the center points of the experiment in both blocks are shown in Table 4. Metallography and Microstructures Metals Handbook [28] clearly presents the compositions of AISI carbon and alloy steels. In the case of the steel alloy 4140, the composition is given by 0.38–0.43 of C, 0.75–1.00 of Mn, a P maximum of 0.035, a S maximum of 0.040, 0.20–0.35 of Si, 0.80–1.10 of Cr, and 0.15–0.25 of Mo.

Table 4. Metallography (2% nital, 500×) that explains the center points of the experiment, 1 h at 852.5 °C (1566.5 °F) with water and oil cooling.

	Blocks	Run	Metallography
Water	2	2	
	2	5	
Oil	1	7	
	1	10	

The analysis presents the ANOVA shown in Table 5. The last column of this table shows the *p* - value. The confidence level managed in this experiment is 95%. Therefore, the factors are significant to the response variable when the *p* - value < 0.05. In such case, temperature and time are certainly significant to the hardness of the piece. On the contrary, the interaction “Temperature × Time” is not significant to the response. It is possible

to visualize the level of significance of each factor through the coded coefficients table explained below.

**Table 5.** ANOVA of the experiment and significance of factors.

Source	DF	Adj SS	Adj MS	F-Value	p-Value
Model	5	13,829.7	2765.9	3161.09	0.000
Blocks	1	27.0	27.0	30.86	0.001
Linear	2	13,231.3	6615.6	7560.71	0.000
Temperature	1	28.1	28.1	32.14	0.001
Time	1	13,203.1	13,203.1	15,089.29	0.000
2-Way Interactions	1	1.1	1.1	1.29	0.300
Temperature*Time	1	1.1	1.1	1.29	0.300
Curvature	1	570.4	570.4	651.86	0.000
Error	6	5.2	0.9		
Lack-of-Fit	4	4.7	1.2	4.75	0.181
Pure Error	2	0.5	0.3		
Total	11	13,835.0			

The residual plots of the response (including the normal probability plot) and the test for homogeneity of variance validate the model’s assumptions, shown in Figure 8.

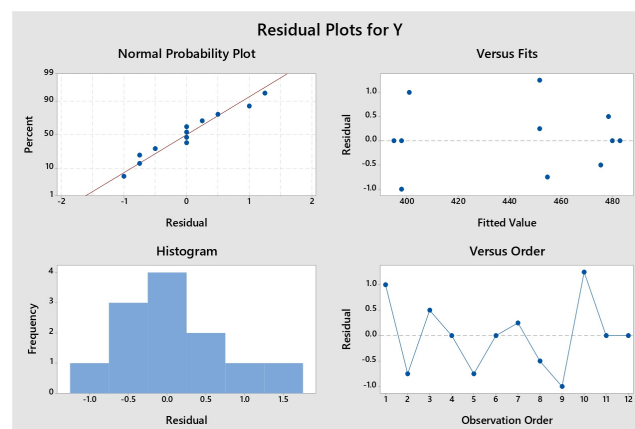


**Figure 8.** The residual plots of the response.

The homogeneity of variance test is shown in Figure 9. It shows evidence of its homogeneity since it has a  $p_{value} = 0.649$ , which is higher than the significance level of  $\alpha = 0.05$ .

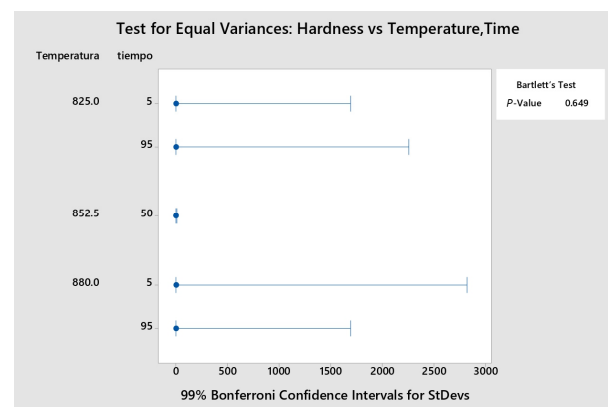


**Figure 9.** Tests for homogeneity of variance of the response hardness.



The mathematical model of this experiment is obtained from Table 6. It is defined by Equation (5).

$$\hat{y} = 438.625 + 1.875 * \text{Temp} + 40.625 * \text{Time} \tag{5}$$

**Table 6.** Coded coefficients table.

Table	Effect	Coefficient	SE Coefficient	t-Value
Constant		438.625	0.331	1326.28
Blocks				
1		−1.500	0.270	−5.55
Temperature	3.750	1.875	0.331	5.67
Time	81.250	40.625	0.331	122.84
Temperature × Time	0.750	0.375	0.331	1.13
Ct Pt		14.625	0.573	25.53

For each unit of change in the temperature, there will be a change in the response variable of 1.875 if the “time” remains constant. Similarly, for the other factor, for each unit of change in time, there will be a change in the response variable of 40.625 if the “temperature” remains constant. After obtaining and analyzing this mathematical model, the steepest path can now be built in an ascending direction considering only significant and individual terms.

The main factor that is selected as the step size  $\Delta x_i$  is “time” because it has the highest absolute regression coefficient in the model. Table 7 shows the step size of factors in natural units.

**Table 7.** The step size of the system from coded to natural units.

Coded	Temperature (°C)	Time (s)
	Natural	Natural
−1	825	5
0	852.5	50
1	880	95

In the case of the factor “temperature”, it is necessary to compute Equation (2) to build the path, as shown in Table 8. The steepest ascent path is the one in which the temperature increases  $\Delta x_1 = 0.0282$  and the time increases in a single natural step  $\Delta x_2 = 1$ , as proposed.

**Table 8.** Computations to establish the step size  $\Delta x_i$  of factors in the steepest path.

	Step Size	
	$\Delta x_1$ for Temperature	$\Delta x_2$ for Time
Natural	0.0282	1.0000
Coded	0.0010	0.0222
Time		
	Coded	Natural
	1	45
	0.0222	1

It is possible to visualize the sequential increments of factors from one region to another through individual experimentation in each step. The block “water” was the cooling environment used to build the steepest path since it is the best level of the block.

The steepest path and the responses are illustrated in Table 9. As previously mentioned, the steepest path is built using the regression model of the designed experiment. In this

case, the path of the steepest direction is intended to find the maximum response from the regression function of the experiment by using an adequate step size to properly change the level of the factors to obtain the proper responses. The moment to stop is determined by the three applied SRs: the MKSR, the ERPSR, and the ASSR.

**Table 9.** Steepest ascent path with individual experiments.

Step	$\Delta$ Temperature	$\Delta$ Time	$Y_i$
0	852.50	50.00	455.00
1	852.53	51.00	456.00
2	852.56	52.00	455.00
3	852.58	53.00	458.00
4	852.61	54.00	457.00
5	852.64	55.00	460.00
6	852.67	56.00	461.00
7	852.70	57.00	458.00

The application of the MKSR is illustrated in Table 10. The limits of the confidence interval are  $a = -b = -2.207$ . The calculation of these limits was made with a  $\kappa = 10$  and a  $\sigma_\epsilon = 0.9$ . Therefore, individual experimentation all along the steepest direction stops when Equation (3) is fulfilled. In other words, experiments stops when  $y(n_i) - y(n_{i-1}) \leq -2.207$ . This happens in step number 7, so the response returns to  $t^* = 6$  when  $\hat{y}_{max} = 461$  units.

**Table 10.** Steepest ascent path with individual experiments and the MKSR.

Step	$\Delta$ Temperature	$\Delta$ Time	$Y_i$	$y(n_i) - y(n_{i-1})$	Significance Test	Decision
0	852.50	50.00	455.00	-	-	Starts
1	852.53	51.00	456.00	1.00	$a < 1 < b$	Continues
2	852.56	52.00	455.00	-1.00	$a < -1 < b$	Continues
3	852.58	53.00	458.00	3.00	$b < 3$	Continues
4	852.61	54.00	457.00	-1.00	$a < -1 < b$	Continues
5	852.64	55.00	460.00	3.00	$b < 3$	Continues
6	852.67	56.00	461.00	1.00	$a < 1 < b$	Continues
7	852.70	57.00	458.00	-3.00	$-3 < a$	Stops

The graph of responses  $Y_i$  is shown in Figure 10.

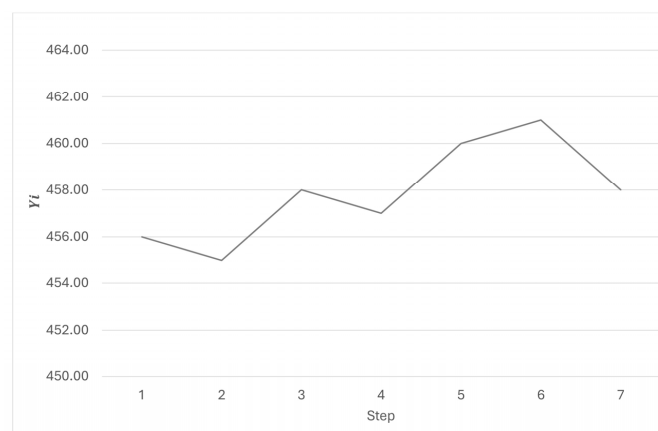


**Figure 10.** Hardness test responses applied to the specimen.

Next, the ERPSR is applied. Recursive estimation is shown in Table 11. The recursive estimation of  $\theta_i^{(t)}$  requires an estimation of the number of individual experiments needed

to reach the improvement, similar to what happens in the MKSR with  $\kappa$ . The estimation needed in this ERPSR is known as  $t_{prior}$ . The number used in this case was  $t_{prior} = 10$ . Experimentation stops when  $d'_t\theta^{(t)} < -1.645\sigma_\epsilon\sqrt{d'_tP_t d_t}$  and the response  $\hat{y}$  returns to  $t^*$  such that  $y(t^*) = \max_{(l=1,\dots,t)}y(l)$ .

**Table 11.** Computations for the enhanced rule (ERPR) for steps  $t < N - 1$ .

$t$	$y(t)$	$\theta_0^{(t)}$	$\theta_1^{(t)}$	$\theta_2^{(t)}$	$P_t$			$d'_t\theta^{(t)}$	$\sigma_\epsilon^2 d'_t P_t d_t$	$-1.645\sigma_\epsilon\sqrt{d'_t P_t d_t}$	Decision
0	455.00	453.250	40.668	-2.033	1	0	0	40.6682	0.6875	-1.3640	Starts
					0	1	0				
					0	0	10				
1	456.00	450.49	37.91	-29.64	0.9	-0.1	-0.8	-21.3664	4.8654	-3.6285	Stops

In  $t^* = 1$ , experimentation stops because  $-21.3664 < -3.6285$  and the improved response goes to  $\hat{y}_{max} = 456$  units.

Finally, the ASSR is applied. After performing experiments on  $t_j, j = 1, 2, \dots, n$  to obtain the observations  $y(t_j)$ , deltas  $\Delta y(t_j) = y(t_j) - y(t_{j-1})$  are as obtained, as seen in Table 12.

**Table 12.** Steepest ascent path with individual experiments and the ASSR.

Step	Temperature	Time	$Y_i$
0	852.50	50.00	455.00
1	852.53	51.00	456.00
2	852.56	52.00	455.00
3	852.58	53.00	458.00
4	852.61	54.00	457.00
5	852.64	55.00	460.00
6	852.67	56.00	461.00

After that, a sample size of  $m = 5$  for  $\Delta Y^{(k)}(t_j)$  is considered:

$$\Delta Y^{(1)}(t_j) = [\Delta y(t_1)] = [1]$$

$$\Delta Y^{(2)}(t_j) = [\Delta y(t_1), \Delta y(t_2)] = [1, -1]$$

$$\Delta Y^{(3)}(t_j) = [\Delta y(t_1), \Delta y(t_2), \Delta y(t_3)] = [1, -1, 3]$$

$$\Delta Y^{(4)}(t_j) = [\Delta y(t_1), \Delta y(t_2), \Delta y(t_3), \Delta y(t_4)] = [1, -1, 3, -1]$$

$$\Delta Y^{(5)}(t_j) = [\Delta y(t_1), \Delta y(t_2), \Delta y(t_3), \Delta y(t_4), \Delta y(t_5)] = [1, -1, 3, -1, 3]$$

$$\Delta Y^{(6)}(t_j) = [\Delta y(t_2), \Delta y(t_3), \Delta y(t_4), \Delta y(t_5), \Delta y(t_6)] = [-1, 3, -1, 3, 1]$$

It is important to assume that  $\Delta Y^{(k)}(t_j)$  is described by a Wiener process to incorporate Hjorth's rate and its parameters  $\beta, \delta$ , and  $\theta$ .

After this procedure, the experimentation scheme with Bayesian inference using the software OpenBUGS is modeled to estimate the parameters  $(\hat{\delta}^{(k)}, \hat{\theta}^{(k)}, \hat{\beta}^{(k)}, \hat{\sigma}^{(k)})$  for each  $\Delta Y^{(k)}(t_j)$  and to characterize the shape of the trajectory for each set  $\Delta Y^{(k)}(t_j)$  according to  $(\hat{\delta}^{(k)}, \hat{\theta}^{(k)}, \hat{\beta}^{(k)})$ , as shown in Table 13.

**Table 13.** Sequences and rate types of  $\Delta Y^{(k)}(t_j)$  for parameter computations.

Sequence k = 1, $y(t_1) = 456$		Sequence k = 2, $y(t_2) = 455$	
$\Delta Y^{(1)}(t_j) = [\Delta y(t_1)]$	[1]	$\Delta Y^{(2)}(t_j) = [\Delta y(t_1), \Delta y(t_2)]$	[1, -1]
Set of parameters	Value	Set of parameters	Value
$\hat{\beta}$	4.27	$\hat{\beta}$	0.28
$\hat{\delta}$	1.04	$\hat{\delta}$	0.07
$\hat{\sigma}$	91.57	$\hat{\sigma}$	1.96
$\hat{\theta}$	38.55	$\hat{\theta}$	0.03
$\hat{\beta}x\hat{\theta}$	164.72	$\hat{\beta}x\hat{\theta}$	0.01
Parameter condition	Trajectory type	Parameter condition	Trajectory type
$0 \leq \hat{\delta}^{(k)} \leq \hat{\theta}^{(k)}\hat{\beta}$	Bathtub-shaped trajectory	$\hat{\delta}^{(k)} \geq \hat{\theta}^{(k)}\hat{\beta}^{(k)}$	Increasing trajectory
Sequence k = 3, $y(t_1) = 458$		Sequence k = 4, $y(t_2) = 457$	
$\Delta Y^{(1)}(t_j) = [\Delta y(t_1)]$	[1, -1, 3]	$\Delta Y^{(2)}(t_j) = [\Delta y(t_1), \Delta y(t_2)]$	[1, -1, 3, -1]
Set of parameters	Value	Set of parameters	Value
$\hat{\beta}$	0.01	$\hat{\beta}$	0.41
$\hat{\delta}$	0.37	$\hat{\delta}$	0.00
$\hat{\sigma}$	0.52	$\hat{\sigma}$	0.50
$\hat{\theta}$	0.17	$\hat{\theta}$	0.02
$\hat{\beta}x\hat{\theta}$	0.00	$\hat{\beta}x\hat{\theta}$	0.01
Parameter condition	Trajectory type	Parameter condition	Trajectory type
$\hat{\delta}^{(k)} \geq \hat{\theta}^{(k)}\hat{\beta}^{(k)}$	Increasing trajectory	$0 \leq \hat{\delta}^{(k)} \leq \hat{\theta}^{(k)}\hat{\beta}$	Bathtub-shaped trajectory
Sequence k = 5, $y(t_1) = 460$		Sequence k = 6, $y(t_2) = 461$	
$\Delta Y^{(1)}(t_j) = [\Delta y(t_1)]$	[1, -1, 3, -1, 3]	$\Delta Y^{(2)}(t_j) = [\Delta y(t_1), \Delta y(t_2)]$	[-1, 3, -1, 3, 1]
Set of parameters	Value	Set of parameters	Value
$\hat{\beta}$	0.51	$\hat{\beta}$	1.91
$\hat{\delta}$	0.94	$\hat{\delta}$	0.00
$\hat{\sigma}$	0.40	$\hat{\sigma}$	0.03
$\hat{\theta}$	0.03	$\hat{\theta}$	0.00
$\hat{\beta}x\hat{\theta}$	0.02	$\hat{\beta} \times \hat{\theta}$	0.00
Parameter condition	Trajectory type	Parameter condition	Trajectory type
$\hat{\delta}^{(k)} \geq \hat{\theta}^{(k)}\hat{\beta}^{(k)}$	Increasing trajectory	$0 \leq \hat{\delta}^{(k)} \leq \hat{\theta}^{(k)}\hat{\beta}$	Bathtub-shaped trajectory

Next, the upper limit of a confidence interval estimates the maximum future increment using  $UL_{(\Delta Y^{(k)}(t_j)|\delta,\theta,\beta,\sigma\sqrt{\Delta t})} = Y_0 + \left(\hat{\delta}^{(k)} + \frac{\hat{\theta}^{(k)}}{(1+\hat{\beta}^{(k)})}\right)(t_{j+1}) + 1.96\hat{\sigma}^{(k)}\sqrt{(t_{j+1})}$ . Computations are shown in Table 14. Experimentation stops if  $Y_0 + \left(\hat{\delta}^{(k)} + \frac{\hat{\theta}^{(k)}}{(1+\hat{\beta}^{(k)})}\right)(t_{j+1}) + 1.96\hat{\sigma}^{(k)}\sqrt{(t_{j+1})} = Y_0$ .

**Table 14.** Upper limit of a confidence interval calculated for each sequence.

$k$	$y(t_j)$	$Y_0$	$\left(\hat{\delta}^{(k)} + \frac{\hat{\theta}^{(k)}}{(1+\hat{\beta}^{(k)})}\right)(t_{j+1})$	$1.96\hat{\sigma}^{(k)}\sqrt{(t_{j+1})}$	$UL_{(\Delta Y^{(k)}(t_j) \delta,\theta,\beta,\sigma\sqrt{\Delta t})}$	Decision to Continue or Stop Experimenting
1	456.00	455.00	6.1	253.8	715	Continues
2	455.00	455.00	0.2	6.7	462	Continues
3	458.00	455.00	1.7	2.0	459	Continues
4	457.00	455.00	0.0	2.2	457	Continues
5	460.00	455.00	5.6	1.9	463	Continues
6	461.00	455.00	0.0	0.2	455	Stops

The search stops at  $UL_{(\Delta Y^{(k)}(t_j)|\delta,\theta,\beta,\sigma\sqrt{\Delta t})} = 455$ . At this point,  $UL_{(\Delta Y^{(k)}(t_j)|\delta,\theta,\beta,\sigma\sqrt{\Delta t})}$  for  $(\Delta Y^{(k)}(t_j)|\delta,\theta,\beta,\sigma\sqrt{\Delta t})$  may approximate to  $Y_0$ , so there is no expectation of increase in future values. This is the case of the response  $y(t_j) = 461$ .

### 5. Discussion

The current study is related to a hardness process of the steel alloy 4140 for optimization purposes. The optimization strategy started with the design of the factorial arrangement with the combination of factors and levels of the experiment. The considered variables in this procedure were the temperature of the furnace and the exposition time to a cooling environment, to subsequently measure the hardness of each specimen. A statistical analysis was developed to obtain significance of terms and regression coefficients. The regression coefficients were used to build the RECU. This equation was used to apply the SADM and visualize the steepest path of improvement. It is particularly relevant to detect the proper moment to stop all along this steepest direction.

In this way, the MKSR, the ERPSR, and the ASSR were applied to properly perform individual experimentation all along the path of improvement. Table 15 shows the performance of each of the applied SRs.

**Table 15.** Performance of each of the applied SRs.

Name of the Procedure	Stopping Rule	Steps Needed	Hardness
Myers and Khuri Stopping Rule	MKSR	7	461 HV
Enhanced Recursive Parabolic Stopping Rule	ERPSR	1	456 HV
Adaptive Sequential Stopping Rule	ASSR	6	461 HV

On the one hand, the MKSR assumes that the observed response will have a linear behavior, while the ERPSR is designed to assume both linear and quadratic behavior. Nevertheless, the ASSR has the capability to adapt to the behavior of the response without the need to make assumptions beforehand. In Table 15, it is easy to see that the ERPSR had a poor performance, reaching 456 HV. On the contrary, the MKSR and the ASSR both had a good performance of 461 HV, and the MKSR also had a good performance because the trajectory or behavior of the response tends to be approximately linear, as seen in Figure 7. Nevertheless, the ASSR achieved that performance using fewer steps than the MKSR. The fact that ASSR has a better performance is explained due to its capability of adaptation to any behavior of the experimental response. It does not matter whether the response tends to be linear or quadratic.

### 6. Conclusions

The application of this paper’s method maximized the hardness of the steel alloy considered. After applying the DOE and obtaining significance of factors, the regression equation was obtained to build the path of improvement for the maximization of the response through the SRs applied. In this case, the MKSR reached a maximum response of  $\hat{y}_{max} = 461$  units in seven steps, while the ERPSR reached a maximum value of



$\hat{y}_{max} = 456$  units in one step. Finally, the ASSR reached a maximum number of  $\hat{y}_{max} = 461$  units in six steps. This last rule attained a better performance, as shown in Figure 11.

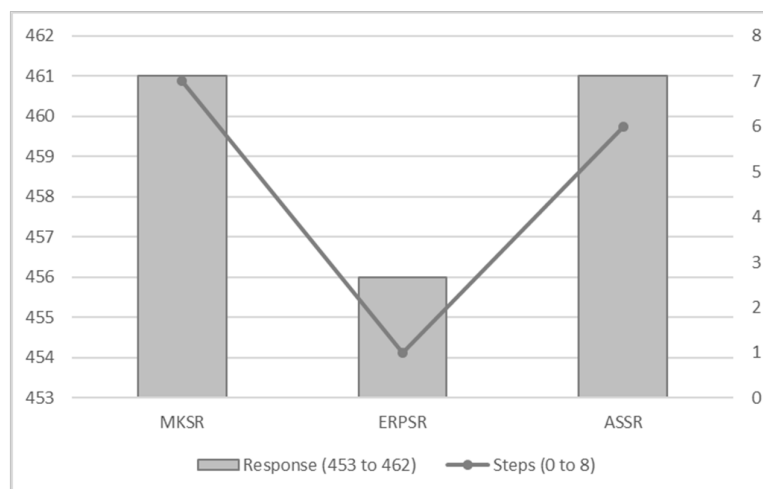


**Figure 11.** Response (hardness) vs. steps needed (to reach that response).

For these types of cases in which a tempering process is related, the recommendation is to use the ASSR along the path of improvement of the steepest ascent if the maximization of the response is the goal. Future research may be feasible using various levels of the factors, different cooling environments, different metal alloys, or even other rules to stop along the improvement.

Overall, these mathematical and statistical methods are essential in industrial applications to analyze data for leading the improvement of efficiency, increasing productivity, pushing performance, and conducting profitability. Its applicability includes the optimization of processes and the enhancement of decision making. The procedures applied in this paper carry broader implications that may include inferential analysis, hypothesis testing, regression analysis, correlation analysis, and Bayesian statistics, among others.

**Author Contributions:** Conceptualization, P.E.G.-N. and L.A.R.-P.; methodology, P.E.G.-N., G.P.-B. and L.A.R.-P.; software, P.E.G.-N. and L.A.R.-P.; validation, P.E.G.-N., G.P.-B., L.A.R.-P. and R.T.-S.; formal analysis, P.E.G.-N., G.P.-B., L.A.R.-P. and R.T.-S.; investigation, P.E.G.-N. and L.A.R.-P.; resources, G.P.-B. and R.T.-S.; data curation, P.E.G.-N., G.P.-B. and L.A.R.-P.; writing—original draft preparation, P.E.G.-N. and L.A.R.-P.; writing—review and editing, P.E.G.-N., G.P.-B., L.A.R.-P. and R.G.-M.; visualization, P.E.G.-N., G.P.-B., L.A.R.-P. and R.G.-M.; supervision, G.P.-B. and R.T.-S.; funding acquisition, L.A.R.-P. All authors have read and agreed to the published version of the manuscript.

**Funding:** This research received no external funding.

**Data Availability Statement:** Dataset available on request from the authors. The raw data supporting the conclusions of this article will be made available by the authors on request.

**Acknowledgments:** It is of high importance to show our deepest appreciation to the “Centro de Investigación en Materiales Avanzados, S.C.” (CIMAV) and all its staff for accepting the development of this experiment in their facilities of Chihuahua city, México. Also, it is essential to express our deepest gratitude to the “Programa para el Desarrollo Profesional Docente” (PRODEP) of the “Dirección General de Educación Superior” (DGESUI) of México.

**Conflicts of Interest:** The authors declare no conflicts of interest.

## References

- Zhang, E.; Zhao, X.; Hu, J.; Wang, R.; Fu, S.; Qin, G. Antibacterial metals and alloys for potential biomedical implants. *Bioact. Mater.* **2021**, *6*, 2569–2612. [[CrossRef](#)] [[PubMed](#)]
- Hoang, A.T.; Tabatabaei, M.; Aghbashlo, M. A review of the effect of biodiesel on the corrosion behavior of metals/alloys in diesel engines. *Energy Sources Part A Recover. Util. Environ. Eff.* **2020**, *42*, 2923–2943. [[CrossRef](#)]

3. Liu, Q.; Zhang, A.; Wang, R.; Zhang, Q.; Cui, D. A review on metal-and metal oxide-based nanozymes: Properties, mechanisms, and applications. *Nano-Micro Lett.* **2021**, *13*, 1–53. [[CrossRef](#)] [[PubMed](#)]
4. Đekić, M.; Ostojić, J.; Sinanović, H.; Korać, F.; Fetić, A.S. Microhardness and corrosion behavior of thermally treated Fe<sub>38</sub>Ni<sub>36</sub>B<sub>18</sub>Si<sub>8</sub> metallic glass. *Met. Mater.* **2023**, *61*, 199–204. [[CrossRef](#)]
5. Gloria, A.; Montanari, R.; Richetta, M.; Varone, A. Alloys for Aeronautic Applications: State of the Art and Perspectives. *Metals* **2019**, *9*, 662. [[CrossRef](#)]
6. Luo, A.A. Recent advances in light metals and manufacturing for automotive applications. *CIM J.* **2021**, *12*, 79–87. [[CrossRef](#)]
7. Zeng, Z.; Stanford, N.; Davies, C.H.J.; Nie, J.-F.; Birbilis, N. Magnesium extrusion alloys: A review of developments and prospects. *Int. Mater. Rev.* **2019**, *64*, 27–62. [[CrossRef](#)]
8. He, X.; Yam, M.C.; Zhou, Z.; Zayed, T.; Ke, K. Inhomogeneity in mechanical properties of ductile iron pipes: A comprehensive analysis. *Eng. Fail. Anal.* **2024**, *163*, 108459. [[CrossRef](#)]
9. Özdemir, M.; Şahinoğlu, A.; Rafighi, M.; Yilmaz, V. Analysis and optimisation of the cutting parameters based on machinability factors in turning AISI 4140 steel. *Can. Met. Q.* **2022**, *61*, 407–417. [[CrossRef](#)]
10. Gürbüz, H.; Gönülaçar, Y.E.; Baday, Ş. Effect of MQL flow rate on machinability of AISI 4140 steel. *Mach. Sci. Technol.* **2020**, *24*, 663–687. [[CrossRef](#)]
11. Murwamadala, R.D.; Rao, V.V. Wear performance of AISI 4140 low-alloy steel PVD coated with TiN. *Adv. Mater. Process. Technol.* **2023**, *10*, 971–987. [[CrossRef](#)]
12. Borchers, F.; Clausen, B.; Eckert, S.; Ehle, L.; Epp, J.; Harst, S.; Hettig, M.; Klink, A.; Kohls, E.; Meyer, H.; et al. Comparison of different manufacturing processes of AISI 4140 steel with regard to surface modification and its influencing depth. *Metals* **2020**, *10*, 895. [[CrossRef](#)]
13. Hunkel, M.; Dong, J.; Epp, J.; Kaiser, D.; Dietrich, S.; Schulze, V.; Rajaei, A.; Hallstedt, B.; Broeckmann, C. Comparative study of the tempering behavior of different martensitic steels by means of in-situ diffractometry and dilatometry. *Materials* **2020**, *13*, 5058. [[CrossRef](#)] [[PubMed](#)]
14. Saraç, E.; Özbek, N.A. Effect of tempering temperature on mechanical properties and microstructure of AISI 4140 and AISI 4340 tempered steels. *Mater. Test.* **2022**, *64*, 832–841. [[CrossRef](#)]
15. Hu, X.; Li, J.; Wang, Z.; Wang, J. A microstructure-informatic strategy for Vickers hardness forecast of austenitic steels from experimental data. *Mater. Des.* **2021**, *201*, 109497. [[CrossRef](#)]
16. Ali, R.; Mehta, P.; Monou, P.K.; Arshad, M.S.; Panteris, E.; Rasekh, M.; Singh, N.; Qutachi, O.; Wilson, P.; Tzetzis, D.; et al. Electrospinning/electrospraying coatings for metal microneedles: A design of experiments (DOE) and quality by design (QbD) approach. *Eur. J. Pharm. Biopharm.* **2020**, *156*, 20–39. [[CrossRef](#)]
17. Smith, J.; Larson, C. Statistical approaches in surface finishing. Part 3. Design-of-experiments. *Trans. IMF* **2019**, *97*, 289–294. [[CrossRef](#)]
18. Moradi, M.; Hasani, A.; Pourmand, Z.; Lawrence, J. Direct laser metal deposition additive manufacturing of Inconel 718 superalloy: Statistical modelling and optimization by design of experiments. *Opt. Laser Technol.* **2021**, *144*, 107380. [[CrossRef](#)]
19. Rao, S. *Engineering Optimization, Theory and Practice*; John Wiley & Sons, Inc.: Hoboken, NJ, USA, 2009.
20. Natrayan, L.; Anand, R.; Kumar, S.S. Optimization of process parameters in TIG welding of AISI 4140 stainless steel using Taguchi technique. *Mater. Today Proc.* **2021**, *37*, 1550–1553. [[CrossRef](#)]
21. Gürbüz, H.; Gönülaçar, Y.E. Optimization and evaluation of dry and minimum quantity lubricating methods on machinability of AISI 4140 using Taguchi design and ANOVA. *Proc. Inst. Mech. Eng. Part C J. Mech. Eng. Sci.* **2021**, *235*, 1211–1227. [[CrossRef](#)]
22. Myers, R.H.; Montgomery, D.C.; Anderson-Cook, C. *Response Surface Methodology, Process and Product Optimization Using Designed Experiments*; John Wiley & Sons, Inc.: Hoboken, NJ, USA, 2009.
23. Myers, R.; Khuri, A. A new procedure for steepest ascent. *Commun. Stat.-Theory Methods* **1979**, *8*, 1359–1376. [[CrossRef](#)]
24. Miró-Quesada, G.; Del Castillo, E. An enhanced recursive stopping rule for steepest ascent searches in response surface methodology. *Commun. Stat. Simul. Comput.* **2007**, *33*, 201–228. [[CrossRef](#)]
25. Del Castillo, E. Stopping rules for steepest ascent in experimental optimization. *Commun. Stat. Part B Simul. Comput.* **1997**, *26*, 1599–1615.
26. García-Nava, P.E.; Rodríguez-Picón, L.A. An adaptive sequential stopping rule for steepest ascent searches based on the Wiener process. *Qual. Technol. Quant. Manag.* **2024**, *1*–23. [[CrossRef](#)]
27. Sanij, M.K.; Banadkouki, S.G.; Mashreghi, A.; Moshrefifar, M. The effect of single and double quenching and tempering heat treatments on the microstructure and mechanical properties of AISI 4140 steel. *Mater. Des.* **2012**, *42*, 339–346. [[CrossRef](#)]
28. Voort, G.F.V.; Lampman, S.R.; Sanders, B.R.; Anton, G.J.; Polakowski, C.; Kinson, J.; Muldoon, K.; Henry, S.D.; Scott, W.W., Jr. *Metallography and Microstructures*; ASM Handbook; ASM International Materials Park: Geauga County, OH, USA, 2004.

**Disclaimer/Publisher's Note:** The statements, opinions and data contained in all publications are solely those of the individual author(s) and contributor(s) and not of MDPI and/or the editor(s). MDPI and/or the editor(s) disclaim responsibility for any injury to people or property resulting from any ideas, methods, instructions or products referred to in the content.